ORIGINAL ARTICLE

CrossMark

A newly green photocatalyst support for azo dye remediation under UV light irradiation

Hayrunnisa Nadaroglu[1,2] · Asghar Lesani[2,3] · Seyedeh Sara Soleimani[2] · Aynur Babagil[2]

Abstract

A new cellulosic material "corn silk" was modified with titanium dioxide nanoparticles as a novel photocatalyst support. In this study, the prepared support was tested for the removal of Reactive Black 5 (RB5) as an azo dye pollutant candidate from synthetic samples. High capability of decolorization (> 99%) was achieved after 30 s using the corn silk/TiO_2 photo-biocatalyst. The effect of important parameters such as pH of the medium, the amount of photocatalyst, mixing rate and dye concentration was investigated and modified. UV–Vis spectroscopy, scanning electron microscopy (SEM), X-ray powder diffraction and Fourier-transform IR spectrometry were applied to characterize the effect of functionalization, structure, surface morphology and photocatalyst properties of the support and mineralization of pollutants. It was observed that the maximum decolorization of RB5 occurred at pH 3.0, 25 °C, 300 rpm, 30 s using the corn silk/TiO_2 composite material for this study. The results reveal that corn silk/TiO_2 composite has high and significant photocatalytic activity.

Keywords Corn silk · Titanium (IV) oxide NPs · Textile dye · Reactive Black 5 · UV photodegradation

Introduction

Excessive production of pollutants with increasing rate threatens the global environment seriously. On the other hand, by increasing public awareness, revolutionary approach to overcome to the problems of the environment is taking place. Finding appropriate solutions and valuable ideas that utilize economic policies, healthy and environmentally friendly methods, without destructive side effects with maximum response in removing pollutants of ecosystem is on the agenda of scientists. Among the wide spectrum of environmental pollutants, especially water contaminants, textile dyes have a larger stake. Remediation of dye-contaminated wastewater released from the textile and other dye industries is necessary to prevent pollution of soil, surface and ground water (Erturk 2010).

More than 0.7 million tons of organic dyes are produced each year globally. It is noted that there are over 10,000 commercially accessible dyes that are classified by their utilization fields, namely acid, reactive, disperse, vat, metal complex, mordant, direct, basic and sulfur dyes. Reactive dyes have been identified as the most environmentally problematic compounds in textile dye effluents for several reasons. First, reactive dyes are intensively used due to their preferable performance and their increasing market share. Second, they are very soluble and approximately 10–15% of the weight of applied reactive dyes is discharged from the dye houses. Third, conventional wastewater treatment units, which reliance on sorption and aerobic biodegradation, have a low removal output for reactive and other anionic soluble dyes. Consequently, they cause to be colored water channels and public complaints, and the pollutants are being transferred to another phase and not being eliminated (Dojcinovic et al. 2012).

Currently, various methods such as physical, chemical, physicochemical and biological treatments (Erturk 2010; Dojcinovic et al. 2012; Laohaprapanon et al. 2015), advanced oxidation (Wu et al. 2008) and electrochemical oxidation such as anodic oxidation (Dhaouadi et al. 2009) and electro-Fenton processes (Ramirez et al. 2013) are used to decolorization of this wastewater. Biological techniques

✉ Hayrunnisa Nadaroglu
  hnisa25@atauni.edu.tr; hnisa25@yahoo.com

1   Department of Food Technology, Erzurum Vocational
    Training School, Ataturk University, 25240 Erzurum, Turkey

2   Department of Nano-Science and Nano-Engineering, Faculty
    of Engineering, Ataturk University, 25240 Erzurum, Turkey

3   Department of Applied Chemistry, Faculty of Chemistry,
    Tabriz University, Tabriz 51666-14766, Iran

are the most common used methods in textile industries as they have low processes cost. Nevertheless, due to complex molecular structure of dyes, aerobic degradation can only remove lesser degree of color. In addition, poor anaerobic degradation of azo dye releases toxic and potentially carcinogenic aromatic amine compounds in the treated waste (Laohaprapanon et al. 2015).

Enzymatic process is another method used for the removal of dyes. However, this technique is not effective as enzymes are inhibited at different pHs, temperatures and by inhibitors (Yanmis et al. 2013). Advanced oxidation processes (AOPs) are widely recognized as highly effective methods for obstinate wastewater treatment. AOPs destroy organic pollutants by forming hydroxyl radicals (Shoabargh et al. 2014). Titanium dioxide nanoparticles have attracted particular interest in AOPs due to their wide applications in various fields and extra benefits such as low cost, high photocatalytic activity and high stableness in comparing with other photocatalysts such as SnO_2 and ZnO (Shoabargh et al. 2014). Immobilization of nanoparticles on a proper support can avoid the requirement for the separation of the surplus amount of photocatalyst from sewage. Supports may be organized into macro-particles, such as sand and glass beads (Khataee et al. 2009), glass tubes surrounding the light source in photoreactor (Ling et al. 2004) and some polymers (Mahmoodi et al. 2006; Kasanen et al. 2011).

Cellulosic materials can be a good support for immobilization of photosensitive nanoparticle, such as TiO_2, ZnO and SnO_2 due to their porosity, abundance, low cost, ease of usage, nontoxic, reusability and replacement. Despite these advantages, application of cellulosic material as support has been understudied. *Luffa sponge* as a cellulosic source was introduced and modified by ZnO nanoparticles (Nadaroglu et al. 2017). In here, we report the immobilization of TiO_2 NPs on corn silk as a novel cellulosic photosensitive support. Corn silk is a fibrous, biodegradable and nontoxic material. We investigated the effect of operational parameters, including dye concentration, mixing speed, amount of CS/TiO_2 nanophotocatalyst and pH on dye decolorization. Moreover, to evaluate the performance of prepared photosensitive support, decolorization of Reactive Black 5 under UV-C irradiation was studied in batch reactor and compared with previously reported processes.

Materials and methods

Chemicals

Reactive Black 5, hexadecyltrimethylammonium bromide (CTAB), hydrochloride acid (HCl), sodium hydroxide (NaOH), sodium hypochlorite (NaClO), titanium dioxide nanoparticles (TiO_2) (< 20 nm) were purchased from
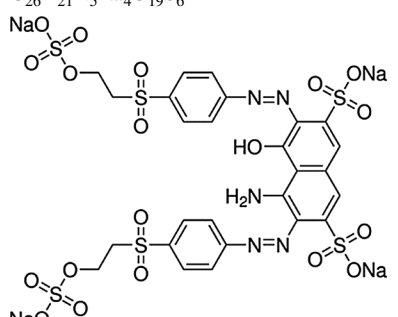
Sigma-Aldrich Chemical. All the chemicals were used without further purification. Distilled water was used for all the tests (GFL 2004). Characteristics and structures of RB5 are summarized in Table 1.

Apparatus

The UV–Vis spectra of dye solutions were recorded from 300 to 900 nm using an Epoch Microplate Spectrophotometer. Decolorization of dye was determined by flowing the dye concentration using their maximum absorbance (597 nm) in a UV–Vis spectrophotometer (Epoch Microplate Spectrophotometer). pH of samples was adjusted by Crison model pH meter. Immobilization of TiO_2 nanoparticles on the texture of corn silk was performed in the Ultrasonic bath (Kudos SK 10GT Model). Bachman Coulter model centrifuge was used to separate the solid photocatalyst from solution. The photocatalytic degradation of RB5 on the CS immobilized nano-TiO_2 was performed under a 15 W/50 HZ UV-C lamp. The distance between the lamp and the phocatalyst reactor was 15 cm. The surface morphology of CS, TiO_2, CS/TiO_2 NPs and $CS/TiO_2/RB5$ was monitored by scanning electron microscope (Zeiss Sigma 300 field emission SEM). X-ray diffractometer (XRD) of CS and TiO_2 IML-CS, before and after dye treatment, was undertaken using a PANalytical Empyrean model XRD at Cu-Kα radiation ($\lambda = 1.54$ Å). The analysis of dried CS, TiO_2 NPs-IML-CS and TiO_2 IML-CS/RB5 was carried out by continuous scans from 10° to 100° at 2° scan rate at 2θ min^{-1} in ambient pressure.

FTIR analysis of RB5 dye, TiO_2 and IML-CS with TiO_2 NPs, before and after tests, was recorded using Vertex 80 Model FTIR Frontier spectrophotometer with attenuated total reflection (ATR) technique in the 4000–400 cm^{-1} region.

Table 1 General characteristics of Reactive Black 5 dye

Reactive Black 5 (RB15)	
Chemical formula	$C_{26}H_{21}N_5Na_4O_{19}S_6$
Chemical structure	
Molar mass (g mol^{-1})	991.82
λmax (nm)	597

Supply and preparation of corn silk

Corn silk was supplied from local vendors. 25 g corn silk sample was weighed and added to 250 mL, 0.5 M NaClO solution. Then, this mixture was treated in a water bath (80 °C) for 1 h. Corn silk was washed thoroughly with 500 mL of pure water and then incubated in the same conditions with 1 M NaOH solution. Then, corn silk was completely washed with double distilled water and dried in oven at 60 °C for 8 h. The dried corn silk sample was fractionated with pure water in a steel blender. 0.02 g TiO_2 NPs was then added to the obtained mixture and treated for 2 h in an ultrasonic bath at 60 °C for immobilizing TiO_2 nanoparticles onto the cellulosic structure of corn silk. TiO_2 immobilized corn silk was separated from the supernatant and washed 5 times with distilled water to remove unbound TiO_2 NPs. The TiO_2 immobilized corn silk support was dried in oven at 60 °C for 8 h and used in all the experiments.

Preparation of dye solutions

The stock solutions of RB5 were prepared in 50 mg L^{-1} concentration and diluted with deionized water. The pH of the solution was adjusted with diluted HCl or NaOH solutions.

Experiments procedure

Reactive Black 5 azo dye degradation was carried out in a closed system consisting of a magnetic stirrer and UV-C lamp (Fig. 1). For this purpose, the reaction medium was prepared by adding 250 mL (50 mg L^{-1}) RB5 azo dye and 0.4 g of TiO_2 NPs–CS catalyst in a 250 mL beaker. The same procedures were performed in CS samples. Distilled water was used as a blank sample. The dye removal efficiency was calculated using the following equation:

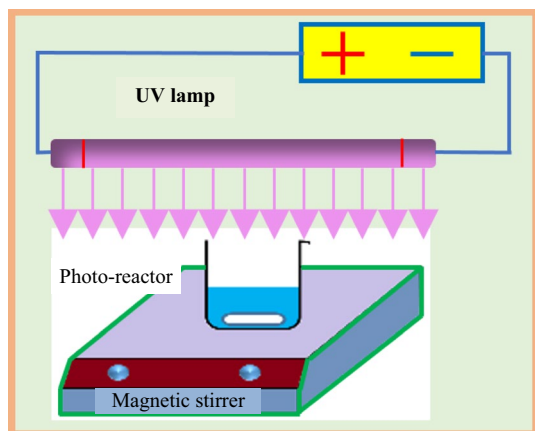$$Removal(\%) = \frac{C_0 - C_t}{C_0} \times 100 \tag{1}$$

Fig. 1 Schematic diagram of batch photoreactor setup

Removal (%) is dye removal efficiency, C_0 (mg L^{-1}) is the initial dye concentration, and C_t (mg L^{-1}) is concentration of dyes at t time.

Effect of various parameters on dye removal

Degradation of RB5 dye was monitored by measuring absorbance at 597 nm. In order to determine the contact time, photodegradation reaction in UV system was followed for 10 min. Samples were taken at regular intervals from the reaction medium, measured against distilled water and degradation % was calculated using Eq. (1).

Also, the effects of stirring speed and medium pH on the photodegradation of RB5 were investigated. For this purpose, pH of RB5 azo dye was adjusted using 0.01 N HCl/NaOH solutions in the range of 3–10. At each pH, the change in absorbance was monitored at 597 nm by establishing the same experiments.

Effect of stirring rate

To study the effect of stirring speed on degradation of dye, 0.4 g corn silk was added to 25 mL RB5 azo dye at 50 mg L^{-1} concentration solution and reactions were occurred at 25 °C pH 3.0 at 100, 200 and 300 rpm. Absorbance was recorded for each speed at 597 nm against distilled water.

## Effect of amount of support material

The different reactions were performed to investigate the effect of support material onto decolorization of RB5 using 0.1 and 0.8 g TiO_2 NPs-IML-CS.

Effect of dye concentration

The effect of dye concentration on the photocatalytic degradation of RB5 azo dye was investigated by setting up the reactions using the same conditions (pH 3.0, 25 °C, 300 rpm) and at the broad spectrum of RB5 dye concentrations: 25, 50, 75, 100, 150 and 200 mg L^{-1}.

## Reusability tests for TiO_2 NPs immobilized corn silk

The elimination of RB5 was performed in the presence of 0.4 g CS/TiO_2 NPs photocatalyst in 10 cycles reactions to assess the potential reusability of TiO_2 IML-CS-NPs at an initial dye concentration of 50 mg L^{-1}. Before each cycle, TiO_2 IML-CS-NPs pieces were washed three times with distilled water. All experiments were carried out in triplicates, and the data are presented as mean value.
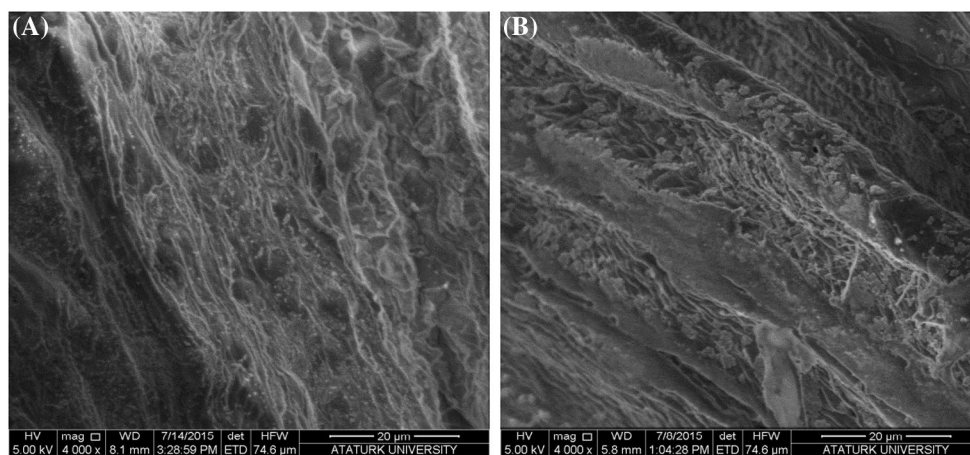
Fig. 2 SEM images of TiO_2 nanoparticles immobilized corn silk before (**a**) and after DB15 dye removal (**b**)
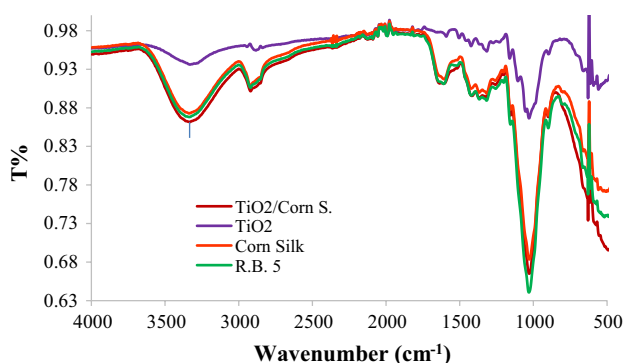
Fig. 3 FT-IR spectra of the CS; TiO_2 NPs; TiO_2 NPs-IML-CS and TiO_2 NPs-IML-CS/RB
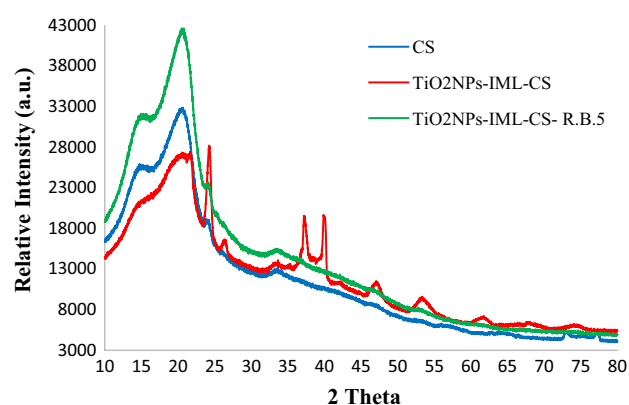
Fig. 4 XRD pattern of CS, TiO_2 NPs, TiO_2 NPs-IML-CS and TiO_2 NPs-IML-CS/RB5

Results and discussion

Characterization of support material

The surface morphology of TiO_2 nanoparticles immobilized corn silk before and after removal of RB5 azo dye samples are given in Fig. 2. It is appeared to be immobilized TiO_2 NPs on the corn silk fibrous structure very well in Fig. 2a. It was also observed from Fig. 2b that the photocatalytic effect of TiO_2 NPs immobilized on CS is very obvious. It is quite clear from Fig. 2b that the degradation of Reactive Black 5 by bio-nanophotocatalyst was carried out successfully.

Figure 3 shows the FTIR spectra of CS, TiO_2 NPs, TiO_2 NPs-IML-CS and TiO_2 NPs-IML-CS/RB5. In the FTIR spectrum of CS, the IR spectra had peaks at 1550–1770 cm^{-1} which was attributed to the C=O stretching and 2800–3000 cm^{-1} which correspond to the ester C=O stretching vibration and carboxylic acid O–H (Miao and Shanks 2011). The peaks at 3330 and 1612.5 cm^{-1} in

the spectra are due to the stretching and bending vibration of the –OH group. In the spectrum of pure TiO_2, the peaks at 560.0 cm^{-1} show stretching vibration of Ti–O and peaks at 1039.6 cm^{-1} show stretching vibrations of Ti–O–Ti (Vetrivel et al. 2014–2015). The FTIR spectrum of TiO_2 NPs-IML-CS after treatment on RB5 shows the peak at 3331, 2922 and 2879.7 cm^{-1}.

The XRD patterns of TiO_2 NPs-IML-CS and TiO_2 NPs-IML-CS + RB5 are depicted in Fig. 4. According to the CSPDS card No. 21-1272, the obtained peak at $2\theta = 25°$ (101) belongs to TiO_2 NPs (anatase) (Theivasanthi and Alagar 2013). Also, at the $2\theta = 32°$, 48°, 55° and 62° peaks are approved that TiO_2 NPs are bound and immobilized to corn silk fibers (Thamaphat et al. 2008; Antic et al. 2012; Ba-Abbad et al. 2012). Based on this evidence by looking at the XRD diagrams of TiO_2 NPs, TiO_2 NPs-IML-CS and TiO_2 NPs-IML-CS/RB5, it was observed that all the immobilized TiO_2 NPs interacted with RB5 azo dye during the photodegradation under UV light. Therefore, all the peaks related

to TiO$_2$ in TiO$_2$ NPs-IML-CS/RB5 were not observed and this event confirmed that the photodegradation is performed.

Effect of reaction time

To confirm the photodegradation of RB5 dye, the absorbance of the samples was monitored at several time points during the photoreaction. As seen from Fig. 5, there was a 99.95% decolorization in the presence of TiO$_2$ NPs-CS-IML in first 30 s. It can be concluded that the immobilized TiO$_2$ NPs onto CS fibers provide the possibility of the degradation of RB-5 dye (50 mg L^{-1}) with high efficiency. When only corn silk was used as the degradation agent, 2 and 5% removal of RB5 azo dye was achieved for 30 and 60 s, respectively. For effective removal of RB5 azo dye at 30 s with TiO$_2$ NPs-IML-CS, there are great benefits such as low cost, energy and time save in industrial scale.

Effect of pH

pH is an important factor for photodegradation reactions taking place on the surface of TiO$_2$ nanoparticles. pH variation can in fact influence the adsorption of dye molecules onto the TiO$_2$ surfaces (Saggioro et al. 2011). The effect of solution pH was studied in a range of 3–10 for the RB5 azo dyes using both CS and TiO$_2$ NPs-IML-CS. Figure 6 shows the variation on the efficiency of the photocatalytic degradation of RB5 at different pHs. Photodegradation was found to be higher in acidic media (pH 3) using TiO$_2$ NPs-IML-CS, with degradation rates of 99%. Up to a pH value of 7, the dye degradation efficiency decreased to 87.66% using TiO$_2$ NPs-IML-CS. Above pH 7, the degradation continued to decrease to about 91.32% at pH 10. But, it was observed that TiO$_2$ NPs-IML-CS was not effected by different pHs too much and it was stable during all remediation of RB5 in all pHs values.

TiO$_2$ NPs-IML-CS surface is positively charged in acidic reaction medium (pH < 7.0), whereas under alkaline
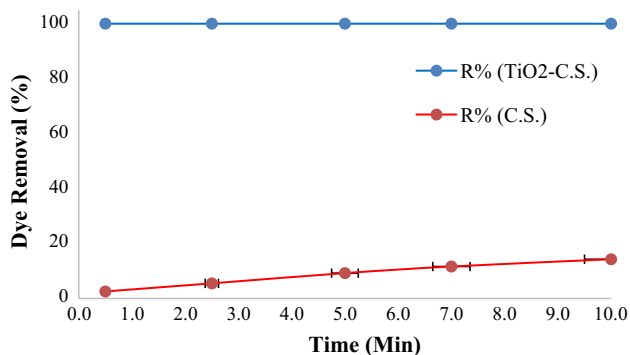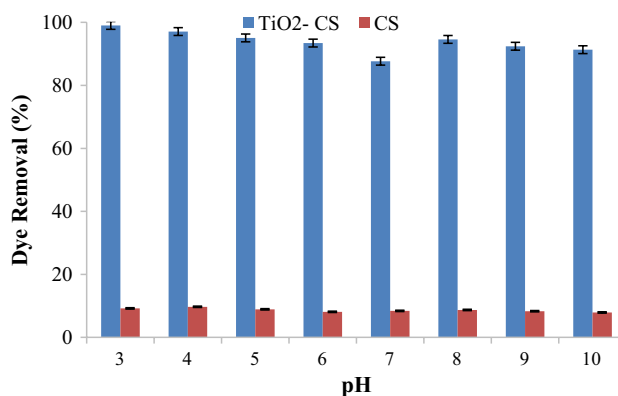
Fig. 6 Effect of pH on the photocatalytic removal rate of RB5 azo dye (25 °C, 300 rpm)

conditions (pH > 7.0) it is negatively charged (Zielinska et al. 2001). Seeing the structure of RB5 azo dye (Fig. 7), a positive charge excess in the TiO$_2$ surface supports a strong interaction with four SO$_3^-$ groups of the dye (Fig. 7a). A negative charge excess promotes the repulsion of the RB5

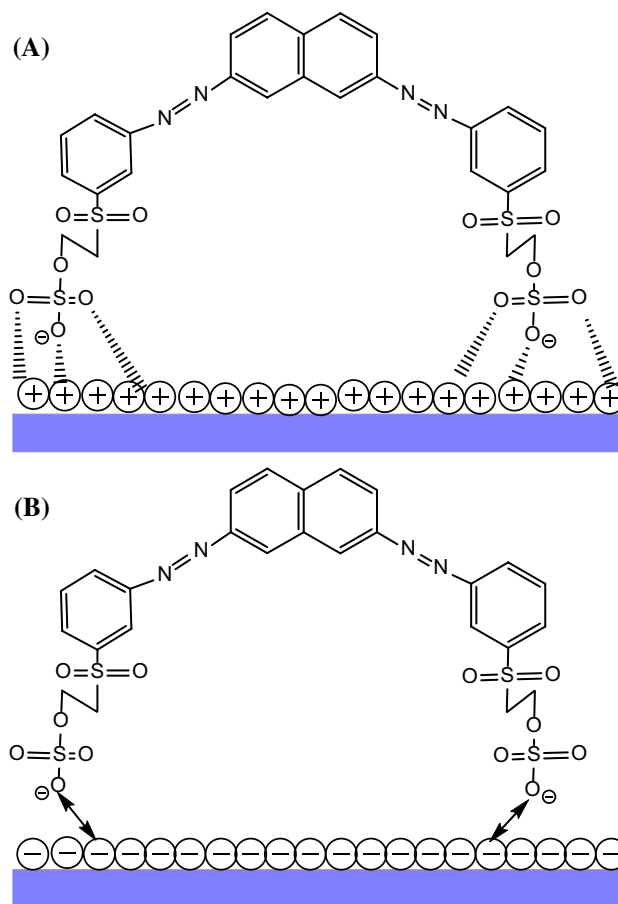**Fig. 7** Schematic reaction mechanism of RB5 and TiO$_2$ NPs-IML-CS **a** acid sites and **b** basic sites

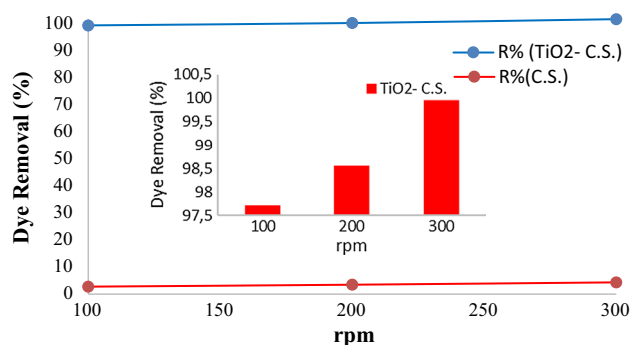**Fig. 5** Photocatalytic removal rate of RB5 50 mg L^{-1} concentration, 25 °C and 300 rpm

azo dye by the TiO₂ NPs-IML-CS surface, reducing the catalytic activity of this photocatalyst (Fig. 7b). These results suggest that the influence of the initial pH of the solution on photocatalysis reaction kinetics is due to the amount of the dye adsorbed on TiO₂ NPs-IML-CS (Zielinska et al. 2001; Saggioro et al. 2011). This hypothesis supports with a reaction occurring at TiO₂ NPs-IML-CS surface and not in the solution, close to the surface.
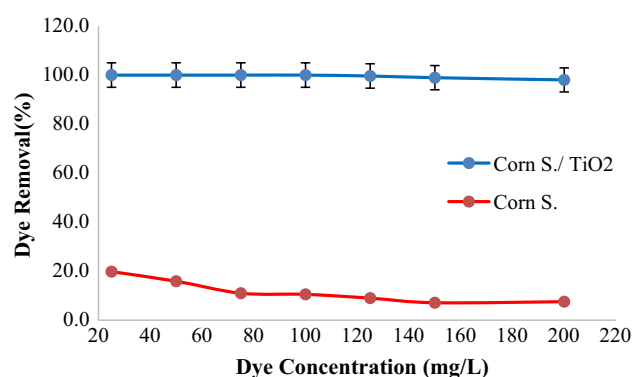
Effect of stirring rate

The effect of stirring rate on the photoelimination reaction of RB5 azo dye was surveyed by changing the speed of mixing from 100 to 300 rpm in dye concentration of 50 mg L⁻¹, contact time 30 s, and temperature 25 °C. As it is shown in Fig. 8, it was found that by increasing the stirring speed, photodegradation of RB5 is increased two units in aqueous solution in the presence of TiO₂ NPs-CS. This increase in degradation of RB5 azo dye reached its maximum at 300 rpm as 99.96% removal rate using TiO₂ NPs-IML-CS. The increase in photodegradation of RB5 might increase the contact between the surface of TiO₂ NPs-IML-CS and RB5 by increasing the stirring speed (Gouvea et al. 2000).

Effect of dye concentration

The effect of the initial concentration of RB5 on the photoelimination of the dye under UV photon was investigated (Fig. 9). As seen in Fig. 9, there is no significant change in the color removal process. When the initial dye concentration decreases from 200 to 50 mg L⁻¹, the removal efficiency of RB5 increases from 98.0 to 100%. These results indicate that the photodegradation rate of RB5 dye with this photocatalyst support is very effective and intriguing. The gradient of the photodegradation performance of RB5 dye by increasing the initial concentration of the dye from 50 to 200 mg L⁻¹ is very feeble.
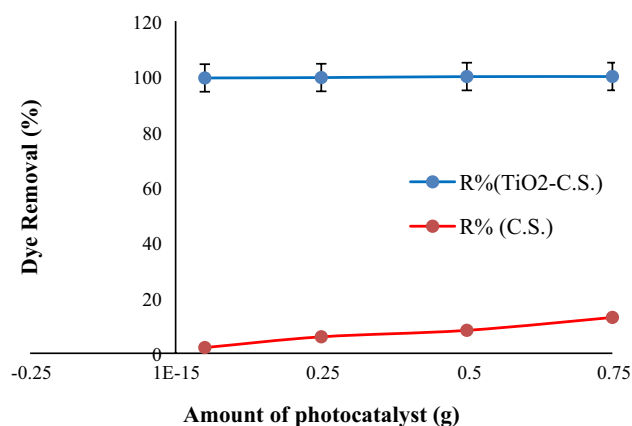

Fig. 9 Effect of dye concentration on the photocatalytic removal rate of RB5 azo dye (pH 3.0, 25 °C, 300 rpm, 30 s)

## Effect of photocatalyst amount on degradation efficiency

The effect of the amount of TiO₂ NPs-IML-CS was also investigated (Fig. 10). The results indicated that by increasing amount of TiO₂ NPs-IML-CS from 0.05 to 0.75 g/50 mL, the removal efficiency of RB5 increases from 89.25 to 99.76%. Using CS and TiO₂ NPs-IML-CS, RB5 with 0.4 g/50 mL of photocatalyst showed a degradation rate of 7 and 99.76%, respectively. It was observed that the efficiency of photodegradation of RB5 azo dye decreased by increasing the initial amount of photocatalyst (Daneshvar et al. 2003). Most likely, photocatalyst prevented the UV light reaching to the RB5 azo dye.

Reusability of bio-photocatalyst

In order to evaluate the reusability and the decolorization capacity of the prepared Photocatalyst (TiO₂ NPs–CS), a series of experiments were designed and carried out in 10

Fig. 8 Effect of stirring rate on the photocatalytic removal rate of RB5 azo dye (pH 3.0, 25 °C, 30 s)

Fig. 10 Effect of the amount of photocatalyst on the photocatalytic removal rate of RB5 azo dye (pH 3.0, 25 °C, 300 rpm, 30 s)
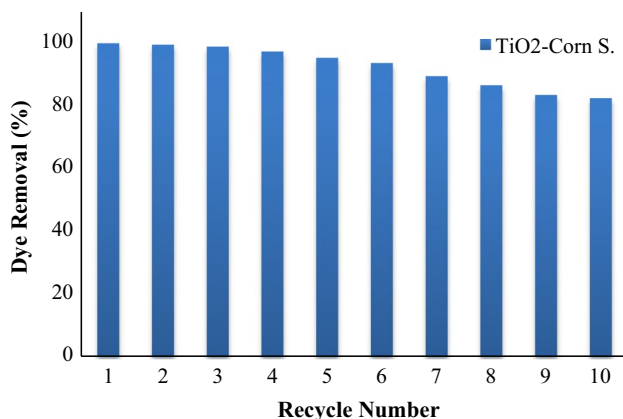
Fig. 11 Effect of reusability capability of TiO_2 NPs-IML-CS on the photocatalytic removal rate of RB5 azo dye (pH 3.0, 25 °C, 300 rpm, 30 s)

cycles (Fig. 11). All parameters including irradiation time (30 s), pH 3.0, RB5 concentration (50 mg L^{-1}) and amount of photocatalyst (0.4 g) were kept constant. The photocatalyst was separated from the solution mixture at the end of each cycle through filtration. The recovered photocatalyst was washed with distilled water and reused in the next degradation cycle. It was found that after 6 cycles, 93.42% removal of RB5 azo dye was obtained. Results showed no significant reduction in photocatalytic performance in photodegrading of RB5 at the first six times; thus, this indicated the stability of TiO_2 NPs-IML-CS as a photocatalyst. At the end of ten degradation cycle, 82.21% of RB5 azo dye was removed. Therefore, based on our results from reusability tests, we can conclude that the dye removal capacity of this novel cellulosic photocatalyst is extremely high.

Conclusion

A novel cellulosic photocatalyst material corn silk–TiO_2 was introduced and successfully applied for degradation of Reactive Black 5 (RB5) as a model azo dye under UV irradiation in batch reactors. High decolorization percentage (99.96%) was achieved in a very short time (30 s). XRD patterns showed the high loaded amount of TiO_2 nanoparticle on cellulosic texture of corn silk and good treated with dye during photoreaction. Based on the UV–Vis and FTIR spectroscopy results, decolorization of RB5 confirmed the cleavage of azo bonds (N=N) of dye molecule. According to these results, the best reaction condition for RB5 degradation (%) was determined as 0.4 g/50 mL TiO_2 NPs-IML-CS, 50.0 mg L^{-1} initial dye concentration, pH 3.0, mix rate 300 rpm and 25.0 °C temperature. The recycling of TiO_2 NPs-IML-CS was performed and found to be adequately

used up to six times. This new photocatalyst, in comparison with others, offers higher quality and efficiency.

References

Antic Z, Krsmanovic RM, Nikolic MG, Marinovic-Cincovic M, Mitric M, Polizzi S, Dramicanin MD (2012) Multisite luminescence of rare earth doped TiO_2 anatase nanoparticles. Mater Chem Phys 135(2–3):1064–1069

Ba-Abbad MM, Kadhum AAH, Mohamad AB, Takriff MS, Sopian K (2012) Synthesis and catalytic activity of TiO_2 nanoparticles for photochemical oxidation of concentrated chlorophenols under direct solar radiation. Int J Electrochem Sci 7:4871–4888

Daneshvar N, Salari D, Khataee AR (2003) Photocatalytic degradation of azo dye acid red 14 in water: investigation of the effect of operational parameters. J Photochem Photobiol A Chem 157:111–116

Dhaouadi A, Monser L, Adhoum N (2009) Anodic oxidation and electro-Fenton treatment of rotenone. Electrochim Acta 54:4473–4480

Dojcinovic BP, Roglic GM, Obradovic BM, Kuraica MM, Tosti TB, Markovic MD, Manojlovic DD (2012) Decolorization of Reactive Black 5 using a dielectric barrier discharge in the presence of inorganic salts. J Serb Chem Soc 77:535–548

Erturk HA (2010) The handbook of environmental chemistry, biodegradation of azo dyes, vol 9. Springer, Berlin Heidelberg, p 1

Gouvea CAK, Wypych F, Moraes SG, Duran N, Nagata N, Peralta-Zamora P (2000) Semiconductor-assisted photocatalytic degradation of reactive dyes in aqueous solution. Chemosphere 40:433–440

Kasanen J, Salstela J, Suvanto M, Pakkanen TT (2011) Photocatalytic degradation of methylene blue in water solution by multilayer TiO_2 coating on HDPE. Appl Surf Sci 258:1738–1743

Khataee AR, Pons MN, Zahraa O (2009) Photocatalytic degradation of three azo dyes using immobilized TiO_2 nanoparticles on glass plates activated by UV light irradiation: influence of dye molecular structure. J Hazard Mater 168:451–457

Laohaprapanon S, Matahum J, Tayo L, You SJ (2015) Photodegradation of Reactive Black 5 in a ZnO/UV slurry membrane reactor. J Taiwan Inst Chem Eng 49:136–141

Ling CM, Mohamed AR, Bhatia S (2004) Performance of photocatalytic reactors using immobilized TiO_2 film for the degradation of phenol and methylene blue dye present in water stream. Chemosphere 57:547–554

Mahmoodi NM, Arami M, Limaee NY, Tabrizi NS (2006) Kinetics of heterogeneous photocatalytic degradation of reactive dyes in an immobilized TiO_2 photocatalytic reactor. J Colloid Interface Sci 295:159–164

Miao SJ, Shanks BH (2011) Mechanism of acetic acid esterification over sulfonic acid-functionalized mesoporous silica. J Catal 279:136–143

Nadaroglu H, Cicek S, Gungor AA (2017) Removing Trypan blue dye using nano-Zn modified Luffa sponge. Spectrochim Acta Part A Mol Biomol Spectrosc 172:2–8

Ramirez C, Saldana A, Hernandez B, Acero R, Guerra R, Garcia-Segura S, Peralta-Hernandez JM (2013) Electrochemical oxidation of methyl orange azo dye at pilot flow plant using BDD technology. J Ind Eng Chem 19:571–579

Saggioro EM, Oliveira AS, Pavesi T, Maia CG, Ferreira LFV, Moreira JC (2011) Use of Titanium dioxide photocatalysis on the remediation of model textile wastewaters containing azo dyes. Molecules 16:10370–10386

Shoabargh S, Karimi A, Dehghan G, Khataee A (2014) A hybrid photocatalytic and enzymatic process using glucose oxidase immobilized on TiO$_2$/polyurethane for removal of a dye. J Ind Eng Chem 20:3150–3156

Thamaphat K, Limsuwan P, Ngotawornchai B (2008) Phase Characterization of TiO$_2$ Powder by XRD and TEM. Kasetsart J Nat Sci 42:357–361

Theivasanthi T, Alagar M (2013) Titanium dioxide (TiO$_2$) nanoparticles-XRD analyses-an insight. Centre for Research and Post Graduate Department of Physics, Ayya Nadar Janaki Ammal College, Sivakasi

Vetrivel V, Rajendran K, Kalaiselvi V (2014–2015) Synthesis and characterization of pure Titanium dioxide nanoparticles by sol–gel method. Int J ChemTech Res 7:1090–1097

Wu CH, Chang CL, Kuo CY (2008) Decolorization of Procion Red MX-5B in electrocoagulation (EC), UV/TiO$_2$ and ozone-related systems. Dyes Pigm 76:187–194

Yanmis D, Bozoglu C, Nadaroglu H, Adiguzel A, Gulluce M (2013) Removal of some textile dyes with laccase from *Anoxybacillus gonensis* (P39). Curr Opin Biotechnol 24:S33

Zielinska B, Grzechulska J, Grzmil B, Morawski AW (2001) Photocatalytic degradation of Reactive Black 5—a comparison between TiO$_2$-Tytanpol A11 and TiO$_2$-Degussa P25 photocatalysts. Appl Catal B Environ 35:L1–L7